NAC-0043_R1

Deep Time Supplemental Analysis for the Clive DU PA

Clive DU PA Model vDTSA1

10 March 2015

Prepared by
NEPTUNE AND COMPANY, INC.

1. Title: Deep Time Supplemental Analysis for the Clive DU PA

2. Filename: Clive DU PA DTSA1 Report R0.docx

3. Description: This report describes details of a supplemental analysis related to the "deep time" component of the *Clive DU PA Model v1.2*. The specific model developed for the Deep Time Supplemental Analysis is the *Clive DU PA Model vDTSA1.gsm*. The analysis provides an approximate evaluation of radon flux at a time after the appearance and retreat of the first intermediate lake to reach the Clive facility.

The model *Clive DU PA Model vDTSA1.gsm* includes site-specific data on depth and age of aeolian deposition. This information is used to replace the distribution used in *Clive DU PA Model vDTSA.gsm* for rate of deposition.

	Name	Date
4. Originator	Ralph Perona, Bruce Crowe, Robert Lee	28 July 2014
5. Reviewers	John Tauxe, Paul Black	5 August 2014
4. Originator Rev 1	Mike Sully, Brice Crowe, Will Barnett, Kate Catlett	6 March 2015
5. Reviewers Rev 1	Paul Black	10 March 2015

6. Remarks

3 March 2015: Revised document (from NAC_0035_R0) with sedimentation data from Dec 2014 field study. Added description of Crowe and Oviatt field studies conducted in December 2014. Added description of distribution development for deposit thickness, age, and correlation. – M. Sully

4 March 2015: Added results from new DTSA model with updated aeolian deposition, *Clive DU PA Model vDTSA1* and reviewed. – K. Catlett

5 March 2015: Paul Black review.

This page is intentionally blank, aside from this statement.

CONTENTS

FIGURES

TABLES

1.0 Deep Time Supplemental Analysis Distribution Summary

The following is a brief summary of input parameter distributions employed in the deep time[1] supplemental analysis (DTSA) that have not previously been documented in other white papers.

For distributions, the following notation is used:

- N(*mean*, *SD*, [*min*, *max*]) represents a normal distribution with mean and standard deviation SD, and optional *min* and *max* if truncation is needed.
- U(*min*, *max*) represents a uniform distribution with minimum *min*, and maximum *max.*
- Beta(α, β, *min, max*) represents a generalized beta distribution with shape parameters α and β, minimum *min,* and maximum *max.*

Table 1. Summary of new distributions for the DTSA

Model Parameter	Value or Distribution	Units	Reference
DepthAeolianDeposition	N(mean = 72.7, SD = 5.0, min = Small, max = Large)	cm	See Section 3.1
AgeAeolianDeposition	Beta($\alpha = 3.318$, $\beta = 7.498$, min = 13,000, max = 15,000)	yr	See Section 3.1
AeolianCorrelationFactor	U(min = 0.5, max = 1.0)	—	See Section 3.1
Sediment_WaterContent	N(mean = 0.253, SD = 0.0215, min = Small, max = total porosity)	—	See Section 3.2
WasteCell_WaterContent	N(mean = 0.133, SD = 0.00532, min = Small, max = 1 - Small)	—	See Section 3.2

"Small" and "Large" are very small and large numbers defined in the Clive DU PA Model.

2.0 DTSA Overview

There are two major components to the Clive depleted uranium (DU) performance assessment (PA) Model v1.2, from which this DTSA model was derived. The first addresses quantitative contaminant fate and transport and subsequent dose assessment for 10,000 years (10 ky) and is based on projections of current societal conditions into the future, and assumes no substantial change in climatic conditions. The second addresses deep time scenario calculations until the time of peak radioactivity. For this analysis, peak radioactivity associated with the ingrowth of progeny from ^{238}U occurs at about 2.1 million years in the future (2.1 My).

[1]Deep time refers to the period between 10 ky to 2.1 My, approximately when the progeny of ^{238}U reach secular equilibrium with ^{238}U.

The DTSA involves projecting the future environment based on the past and is described in the *Deep Time Appendix to version 1.2 of the Modeling Report.* The conceptual model of the past environment underlying the DTSA is based on scientific records (sediment borehole logs, ice cores, deep ocean cores) of the past eight glacial/climate cycles that have lasted approximately 100 ky each. Earth is currently in an interglacial period. The model considers cycles from the near beginning of an interglacial period onwards. In past 100-ky cycles, after the interglacial period, the average temperature drops and average precipitation increases throughout the glacial cycle (typically an 'ice age'), until the relatively cold period ends, and the next interglacial period begins.

The objective of the deep time calculations in the Clive DU PA Model v1.2 is to assess the potential impact of glacial period pluvial lake events on the portion of the Federal Cell that is used for DU disposal (the Federal DU Cell) from 10 ky through 2.1 My post-closure. A pluvial lake is typically associated with extensive glaciation, resulting from low evaporation, increased cloud cover, increased albedo, and increased precipitation in landlocked areas. In effect, the first 10 ky of the Clive DU PA Model v1.2 is projected under interglacial conditions, and the deep time calculations include an evaluation of the effect on DU disposal of future 100-ky glacial cycles for the next 2.1 My. The Clive DU PA Model v1.2 evaluates only that DU disposed in the Federal DU Cell.

Doses to potential human receptors were *not* calculated in the deep time assessment in the Clive DU PA Model v1.2. Calculation of radiological dose at times beyond 10 ky is not required in Utah regulation, which specifies the need for a qualitative assessment with simulations for this period. And, for example, the IAEA (2012) has indicated that calculating doses beyond a few hundred years is not defensible. That is, quantitative dose assessment, particularly subsequent to lake events related to the interglacial cycle, is insupportable from a scientific and technical perspective. However, if deep time modeling results such as radon flux are considered in the context of gauging system performance, such results may provide limited insight into the behavior of the disposal system in deep time. This is the objective of the DTSA.

The deep time assessment in the Clive DU PA Models v1.0 and v1.2 was developed for DU waste disposal configurations in which the waste was placed within the embankment above the grade of the surrounding land surface. Those models simply assumed the embankment would be destroyed by wave action at the return of the first lake to the Clive elevation, and that all waste remaining in the embankment, including that disposed below grade in v1.2, would then be dispersed. Note that due to contaminant fate and transport processes active in earlier time, some radiological constituents will have migrated away from the embankment to groundwater, the atmosphere, and surface soils.

In contrast, the currently proposed waste disposal configuration is that all DU waste will be placed below today's surrounding grade, and will not be subject to dispersal upon return of the first lake. The thickness of aeolian deposits prior to the return of an intermediate lake and the dynamics of wave action become factors in determining the total depth of embankment material and sediment covering the DU waste when the first lake recedes.

Because of the extremely high uncertainty involving the projection of environmental conditions in the very distant future, a series of assumptions that are deemed reasonable are made to arrive at a plausible deep time situation in which the Federal Cell performance can be qualitatively

assessed. However, it should be realized that any number of different events, features, and processes may occur when trying to project conditions 100 ky or longer from today. In the *Deep Time Assessment Appendix* to version 1.2 of the DU PA Model Report, a "deep" lake is defined as a large glacial-period lake on the scale of Lake Bonneville. Such lakes have occurred in several of the past 100-ky climate cycles. An "intermediate" lake is defined as a smaller lake that reaches the elevation of Clive (described further below). These lakes are assumed to occur in the transgressive and regressive phases of a large lake, but evidence of such lakes is difficult to find because deep lakes rework the paleoshorelines. Deep and intermediate lakes are assumed to interact with the Federal DU Cell such that the part of the embankment (or cell) that is above the future surrounding grade is destroyed and hence dispersed in the first lake that reaches the elevation of Clive. Wave action is assumed to disperse the embankment materials as the edge of the lake intersects the site. Following the pattern of the spits from the nearby Grayback Hills, dispersal is not assumed to result in the complete removal of the embankment but rather to disperse the material so that it is spread over some larger area. Dispersal is assumed to leave behind a layer with some nominal thickness; i.e., the embankment is spread out so that its height and slope is decreased. Based on evidence from paleoshorelines, this thickness is assumed to be less than 1 m, but could be more in the center of the embankment.

Upon their advent, wave action associated with transgressing and regressing intermediate lakes reworks the lake-sediment interface to a depth that is controlled by the dynamics of the wave action. Evidence of wave action and sedimentary processes for past levels of Lake Bonneville are preserved in sedimentary and geomorphic features. These include paleoshorelines, fan and river deltas, wave-cut cliffs, bayhead barriers and spits (Sack, 1999; Schofield et al., 2004; Nelson, 2012). The absence of coarse clastic sediments in the described upper layers of the Pit wall of the Clive site (*Deep Time Assessment Appendix to version 1.2 of the Modeling Report* – reproduced here as Appendix A) is consistent with the absence of significant longshore drift and sedimentary activity associated with larger geomorphic landforms such as spits, barriers, alluvial fans, and river deltas. The most relevant lake features from the geologic record are paleoshorelines. Schofield et al., (2004) divide Lake Bonneville shorelines into erosion-dominated and deposition-dominated. The elevation difference between shoreline bench deposits and shoreline fronts from their studies provides a time-integrated analog for the dynamics of wave action during shoreline transgressions and regressions (see Figure 3 in Schofield et al., 2004). These elevation differences are about 90 cm for erosion-dominated shorelines and 40 to 65 cm for deposition-dominated shorelines. Thus, the process of wave action is assumed to remove approximately the same thickness of sediment (½ to 1 m) as the residual embankment thickness described above (<1 m).

Although some embankment thickness and removal of sediment through wave action are expected, they are not modeled explicitly. Instead, these effects are assumed to be relatively small compared to aeolian and lake deposition effects, and are assumed to have roughly a net zero effect on overall sedimentation before and after the return of an intermediate or large lake (remaining embankment thickness is about ½ m and removal depth is about ½ m). The DTSA model thus explicitly considers aeolian and lake deposition only as contributors to sedimentation thickness.

3.0 Estimation of Aeolian Deposition Rate and Time Period to the Next Intermediate Lake

3.1 Aeolian Deposition Rate

Post-Lake Bonneville rates of aeolian deposition are expected to be relatively high in the Clive area because of the large expanses of exposed lake sediments west of the site. Evidence supporting this conclusion includes:

- There are active and vegetated dune fields in the Knolls area west of the Clive site. The Knolls dune field is one of the larger dune fields in the Great Salt Lake Desert dune areas, with gypsum sediments derived from shoreline and lake sediments of Lake Bonneville. The Knoll dune drift directions are variable but are predominantly from the southwest (Jewell and Nicoll, 2011).
- Examination of satellite imagery for the Clive area shows that active sand dunes are 10 km west-southwest of the Clive site. Sand ramp and aeolian deposits extend eastward to the Clive site.
- The upper approximately 70 cm of sediments of the stratigraphic section described at the Clive site is interpreted to be of aeolian origin (see Appendix A of the *Deep Time Assessment v1.2 Appendix*, repeated in Appendix A of this report).

3.1.1 Field Studies

Field studies of the aeolian depositional history at the Clive Disposal Site were conducted in December 2014 to provide information for describing aeolian deposition rates for the DTSA model (Neptune, 2015). The primary goals of the field studies were to evaluate the modern geological and depositional setting of the Clive site, and to assess the stratigraphy of the Holocene and Pleistocene lake sedimentation of Lake Bonneville and post-lake depositional processes within the Clive site including: re-evaluating the stratigraphic section previously described by Oviatt (1985 – cited in Neptune, 2014); describing the aeolian sediments and processes affecting the sediments; measuring variations in thickness of the deposits across the site; and, providing sufficient replicate measurement at multiple sites to estimate aeolian thickness.

The field studies achieved these primary goals, and the replicate measurements of the thickness of aeolian deposits located in the upper part of the stratigraphic section were made at multiple locations on and in the vicinity of the Clive Disposal Site. The data are presented in Neptune (2015), and are used below to develop input probability distribution for the DTSA, as described in Section 3.1.2.1.

3.1.2 Probability Distributions for the Depth and Age of Aeolian Deposition

The DTSA model requires specification of input probability distributions for the depth of aeolian deposition, and the age of the aeolian deposits. Together, these two variables provide the information needed to estimate the rate of aeolian deposition. The distribution for the depth of

aeolian is based on the field data described above (Neptune, 2015), whereas the distribution for the age of the aeolian deposits are derived from a summary paper by Oviatt (2015).

An assumption is made that the aeolian deposition rate has been in steady-state since the regression of Lake Bonneville and will continue in steady-state in the future until conditions at the site change considerably (e.g., natural climate change). The distributions are based on the depth of aeolian deposition since Lake Bonneville regressed past the elevation of Clive and the age at which regression past the Clive elevation occurred. These distributions are used to model future aeolian deposition until the return of a lake at the elevation of Clive.

3.1.2.1 Probability Distribution for the Depth of Aeolian Deposition

The summary statistics of the field thickness measurements provide the information needed to develop a distribution of average aeolian deposition since the regression of Lake Bonneville past the elevation of Clive. The mean is 72.7 cm, and the standard deviation is 16.6 cm. There are 11 data points, and the data are reasonably symmetric about the mean. Consequently, a normal distribution is specified for the DTSA model with a mean of 72.7 cm and a standard error of 5.0 cm. A reasonable simulation range considering ± 3 standard errors would be 57.5 to 87.5 cm. The minimum of the normal distribution was set to a very small number and the maximum was set to a very large number, so that the distribution was not unnecessarily restricted.

This distribution represents spatio-temporal scaling, so that the distribution is of the average depth of aeolian deposition since the Lake Bonneville regressed past the elevation of Clive. This provides a better representation of the future effect of aeolian deposition over long time frames and spatial scales of the DTSA model. The data are reproduced in Table 2 for ease of reference.

Table 2. Thickness Measurements from Field Studies of Aeolian Silt, Clive Disposal Site

Neptune Field Studies December 2014				
Site	**GPS Coord** UTM E	**GPS Coord** UTM N	**Silt Thick** (cm)	**Date** (mm/dd/yy)
Clive 29-1	321354	4508262	90.0	12/16/14
Clive 29-2	321390	4508256	80.0	12/16/14
Clive 29-3	321423	4508248	80.0	12/16/14
Clive 29-4	321502	4508236	60.0	12/16/14
Clive 29-5	321239	4508283	110.0	12/16/14
Clive 5-1	320813	4504729	55.0	12/16/14
Clive 5-2	320869	4504730	70.0	12/16/14
Clive 5-3	320914	4504731	60.0	12/16/14
Clive 5-4	321041	4504732	70.0	12/16/14
Clive Hand-Dug-1	322093	4507482	70.0	12/17/14
Clilve hand-Dug-2	320445	4507035	55.0	12/17/14
		Mean	**72.7**	
		Std Error	**5.0**	

Note that several replicate measurements were taken at each location (usually three or four), and the results presented represent the average thickness at each location. These data are also supported by previous data collected at the Clive Site, which also presented in Neptune (2015), The pedigree of these extra data is not clear and the measurements were not as precise as those made in the Neptune field study, however, the data are supportive of the results of the field study, indicating very similar aeolian depth data. These data provide another 21 data points that have an average of 71 cm depth of aeolian deposits, with a standard error of 4 cm. Because of the uncertain pedigree and lesser precision of these extra data they were not used in the distribution development. Their use would have resulted in a much tighter distribution because of the scaling effects of averaging.

3.1.2.2 Probability Distribution for the Age of Aeolian Deposition

Ages of the deposits were determined from radiocarbon dating. The summary paper by Oviatt (2015) provides the most recent compilation and interpretation of radiocarbon ages for the chronology of Lake Bonneville. Based on information summarized in Figure 2 of Oviatt (2015) and supported by the supplemental radiocarbon data referenced in the paper, the preferred estimate for the age of the final regression of Lake Bonneville below the altitude of the Clive site is about 13,500 yrs B.P. (Clive elevation 1304 m). A reasonable lower bound on the youngest or minimum age for this event is 13,300 years B.P based on radiocarbon ages determined from organic material collected in post-Bonneville wetland deposits (Oviatt, 2015). The reasonable oldest or maximum age of lake regression at the Clive site is constrained by the age of the Provo shoreline and reliable radiocarbon ages for sites above the altitude of the Clive site and below the Provo shoreline. This reasonable maximum age is estimated to be about 14,500 yrs B.P. A distribution was developed based on these values from Oviatt (2015) and on expert elicitation of Oviatt. Oviatt suggested that values around 13,500 years were more likely. Based on this information a beta distribution was fit to approximate elicited quantiles. The following quantile inputs were used:

- Absolute minimum possible age – 13,000 yrs
- Reasonable minimum age – 13,300 yrs
- Most likely age – 13,500 yrs
- Reasonable maximum age – 14,500 yrs
- Absolute maximum possible age – 15,000 yrs

After considering possible quantiles for the middle three terms, a beta distribution fit was agreed upon with the following parameters:

- Minimum – 13,000 years
- Maximum – 15,000 years
- α (shape 1 parameter) – 3.318
- β (shape 2 parameter) – 7.498

This beta distribution has a mean of approximately 13,600 years and a standard deviation of approximately 270 years. The mean is reasonably close to the specified most likely age of 13,500 years. Quantiles of this beta distribution are provided below:

- Quantiles:
  - 2.5% – 13,174 yrs
  - 10% – 13,284 yrs
  - 20% – 13,378 yrs
  - 50% –13,592 yrs
  - 80% – 13,846 yrs
  - 90% – 13,988 yrs
  - 97.5% – 14,207 yrs

The distribution is slightly positively skewed, hence the median is slightly less than the mean, and the difference between the maximum and the median is greater than the difference between the minimum and the median. This distribution is used directly in the Clive DU PA Model vDTSA1.

Note that averaging is not employed for this distribution. The distribution simply reflects the age over which aeolian deposition has occurred. The rate of Aeolian deposition is average for spatio-temporal scaling by dividing the depth of deposition by the age over which deposition has occurred, and is described in the next section.

3.1.2.3 Resulting Distribution for Aeolian Deposition Rate

In principle, the rate of aeolian deposition is the deposition depth divided by the age over which deposition occurs. However, an assumption is made that greater ages imply greater depths, in which case there is a correlation between depth and age of aeolian deposition. There are no data to inform a correlation between these two variables. Although elicitation could be performed to develop a correlation, the approach taken is to specify the correlation as uncertain across a range of 0.5 to 1. In a sense, this distribution is chosen to indicate that the "data are more likely to be correlated than not-correlated". A uniform distribution is used across this range, but this input will be tracked specifically in sensitivity analysis to determine if it is an important predictor of the DTSA model output.

Using the input distributions described in Sections 3.1.2.1 and 3.1.2.2 and the correlation described above, the resulting distribution of rate of aeolian deposition in the DTSA model has a mean of approximately 5.3×10^{-5} m/yr, (roughly 53 cm every 10ky) with a standard deviation of approximately 3.0×10^{-6} m/yr. A histogram of the aeolian deposition rate for 1,000 realizations is depicted in Figure 1. Quantiles from these simulated data include:

- 5% – 4.84E-05 m/yr
- 10% – 4.96E-05 m/yr
- 20% – 5.10E-05 m/yr
- 50% – 5.34E-05 m/yr
- 80% – 5.58E-05 m/yr
- 90% – 5.71E-05 m/yr
- 95% – 5.81E-05 m/yr

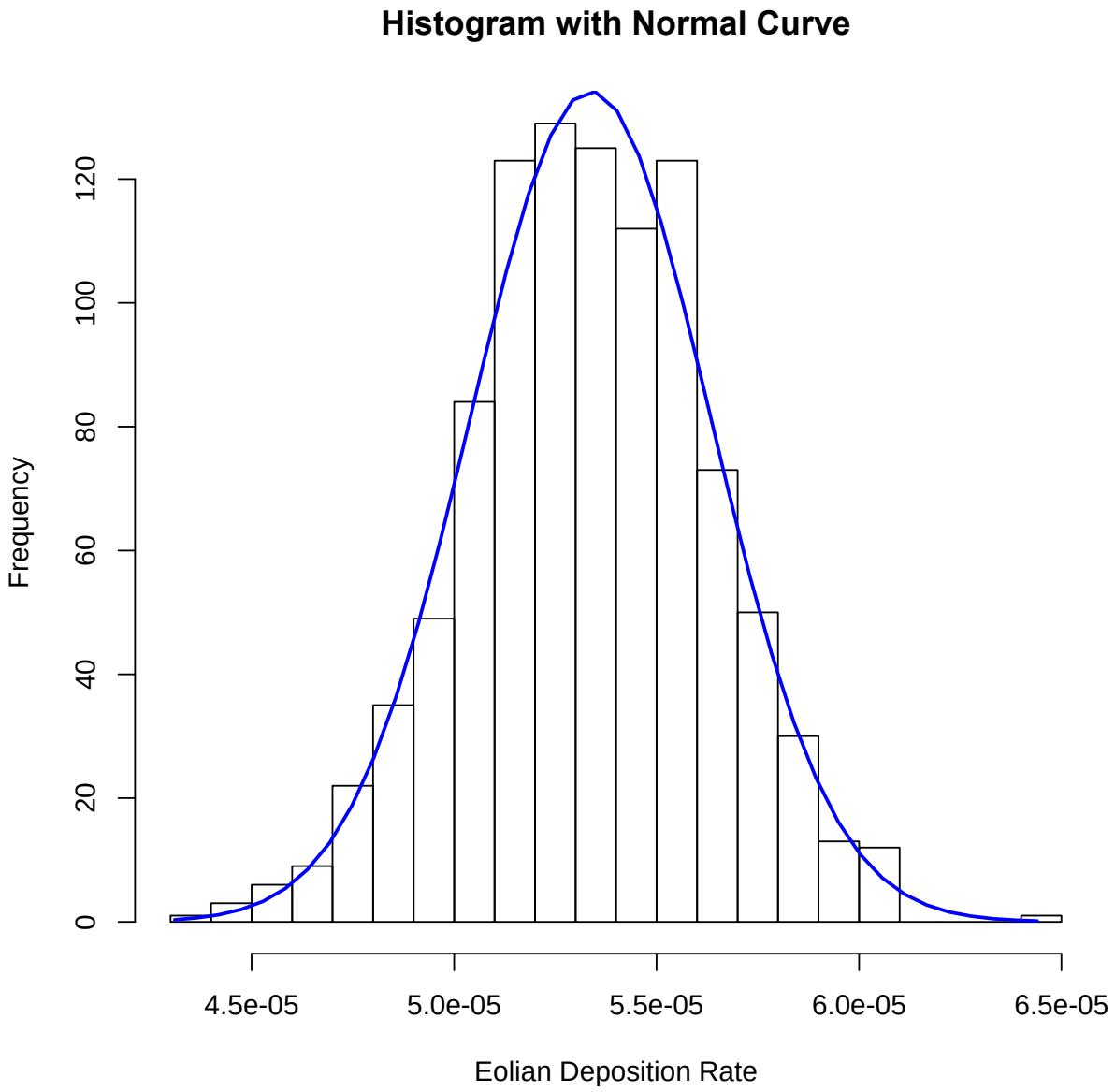

Figure 1. Aeolian deposition rate results for 1,000 realizations from the Clive DU PA Model vDTSA1. Units are m/yr.

The distribution is very symmetric, as evidenced by the normal distribution fit that is laid over the histogram. The normal distribution has the mean and standard deviation as specified above, and the quantiles, which show similar differences between the 95% quantile and the median and the 5th quantile and the median.

Overall, this intermediate product of the DTSA model suggests aeolian deposition rates of a little more than ½ m every 10,000 years.

3.2 Waste and Sediment Water Content

Volumetric water contents are defined for the DU waste, and for sediments overlying the waste, in order to support radon diffusive flux calculations through these sediments. The DTSA input distributions of water contents for these materials are based on a distributions resulting from a large number of model realizations of the Clive DU PA Model v1.2. Figure 2 shows the Unit 4 water content resulting from 10,000 realizations of the model. A normal distribution was chosen to represent these results. The mean for the sediment water content in the DTSA was assigned the same as the mean and standard deviation of this model output distribution, 0.253 and 0.0215, respectively. The minimum of the distribution is "Small" and the maximum is the porosity of Unit 4 sand for that realization.

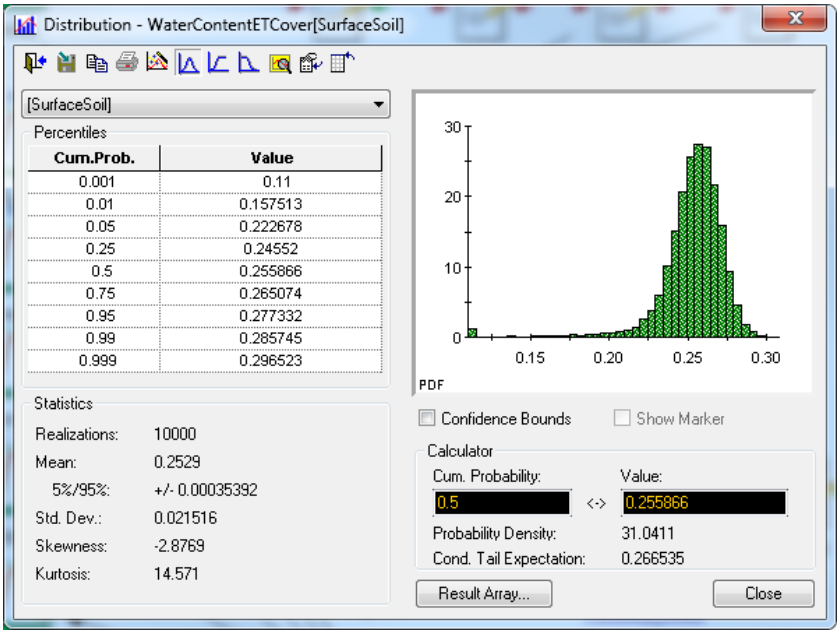

Figure 2. Cover material water content results for 10,000 realizations from the Clive DU PA Model v1.2

A distribution for water content is also derived for the DU waste material from the Clive DU PA Model v1.2. The resulting water content values of the lowermost five waste cells (containing the below-grade DU waste) were exported from the Clive DU PA Model v1.2. Average and standard deviation values were obtained across these five layers, producing a DTSA input distribution for the water content of the waste layer, with a mean of 0.133 and a standard deviation of 0.00532.

3.3 Time Period to the Next Intermediate Lake

For modeling purposes, a distinction is made between shallow, intermediate and deep lakes.

- Deep lakes are assumed to be similar to Lake Bonneville during the Bonneville and Provo shoreline stages, and occur no more than once per 100-ky glacial cycle (this is an assumption of the heuristic model approach described in the *Deep Time Appendix to version 1.2 of the Modeling Report*).

- Intermediate lakes are assumed to be smaller lakes that reach and exceed the elevation of Clive, but are not large (or deep) enough that carbonate sedimentation is the dominant mode of lake deposition. These intermediate lakes are also assumed to be large enough to maintain wave action that will destroy the waste embankment. The transgressive and regressive phases of the Bonneville and Provo shoreline lakes are assumed to be associated with intermediate lakes during the transient phases of the lakes where they exceed the elevation of the Clive site and sedimentation is dominated by clastic deposition associated with wave activity and reworking of lake sediments (see the *Deep Time Appendix to version 1.2 of the Modeling Report* for the chronology of the lake cycles, subject to modifications described below). The Gilbert shoreline provides an example of a lake formed in the regressive phase of Lake Bonneville, although recent research indicates that the Gilbert Lake did not reach the elevation of Clive (Oviatt, 2014).
- Shallow lakes are assumed to exist at all other times. These lakes do not affect the deep time scenarios for the Clive site. The current Great Salt Lake is an example.

The current Great Salt Lake is an example of a shallow lake, as is the Gilbert Lake that is now interpreted to have remained below the elevation of the Clive site (Oviatt, 2014). Under current climate (i.e., interglacial) conditions, it is assumed that only shallow lakes will occur, since an intermediate lake has not occurred since before the Gilbert shoreline was developed over 10 ka (Oviatt, 2014). Under future climate conditions, some glacial cycles will produce a deep lake in the Bonneville Basin, and intermediate lakes will occur during the transgressive and regressive phases of a deep lake, or during glacial cycles that do not produce a deep lake. The timing of the return of the first intermediate lake is important in the DTSA model because it is assumed that the Clive waste disposal embankment is partly destroyed upon the occurrence of the first intermediate lake.

Sedimentation is assumed to occur during these intermediate lake events at greater annual rates than is assumed to occur for the open-water phase of deep lakes. This is based on the pre-Bonneville lacustrine cycles that are documented in the *Deep Time Appendix to version 1.2 of the Modeling Report*. The intermediate lake is assumed to recede after some period of time, at which point a shallow lake relative to the Clive facility will occupy Bonneville Basin until the next intermediate or deep lake cycle. Modeling of radon flux focuses on this point in time.

Tzedakis et al. (2012a) examined the duration of interglacial periods during the last 800 ka. They suggest the onset of interglacials occurs within 2 ky of the boreal summer insolation maximum/precision minimum consistent with Milankovitch forcing. The phasing of precession and obliquity is inferred to control the persistence of interglacials over two insolation peaks of about 13 ka and 28 ka. Given only orbital forcing (i.e., orbital parameters determining glacial periods), the next glacial period could occur as little as 1500 years from now (Tzedakis et al. 2012b) if atmospheric CO_2 concentrations do not exceed 240 ppm. However, numerous studies reviewed by the Intergovernmental Panel on Climate Change (IPCC) have concluded that the next glacial period will not occur for at least 50 ky if CO_2 levels continue to remain above 300 ppm. Chapter 5 of the latest IPCC report (IPCC 2013) states:

> "Since orbital forcing can be accurately calculated for the future…, efforts can be made to predict the onset of the next glacial period. However, the glaciation threshold depends not only on insolation but also on the atmospheric CO_2

> concentration… Models of different complexity have been used to investigate the response to orbital forcing in the future for a range of atmospheric CO_2 levels. These results consistently show that a glacial inception is not expected to happen within the next approximate 50 ky if either atmospheric CO_2 concentration remains above 300 ppm or cumulative carbon emissions exceed 1000 PgC [petagrams of carbon—one petagram is 10^{15} g]. Only if atmospheric CO_2 content was [sic] below the pre-industrial level would a glaciation be possible under present orbital configuration… Simulations with climate–carbon cycle models show multi-millennial lifetime of the anthropogenic CO_2 in the atmosphere… Even for the lowest [emissions] scenario, atmospheric CO_2 concentrations will exceed 300 ppm until the year 3000. It is therefore *virtually certain* [i.e., a greater-than 99% probability] that orbital forcing will not trigger a glacial inception before the end of the next millennium."

Current CO_2 levels are approximately 400 ppm (http://co2now.org/images/stories/data/co2-mlo-monthly-noaa-esrl.pdf), and steadily rising over the past approximately 150 years from anthropogenic sources. Preindustrial levels of CO_2 were about 280 ppm whereas CO_2 levels associated with glacial periods tend to be about 240 ppm (Tzedakis et al., 2012b). It would require major modifications to CO_2 emissions worldwide in order to return to preindustrial levels, and/or engineering solutions (e.g., "scrubbing' or use of iron filings) to remove CO_2 from the atmosphere. The Clive DU PA Model projects current knowledge as a fundamental assumption, therefore it is assumed here that no major interventions will occur, and CO_2 levels will continue to rise, or at least will not decrease to below 300 ppm within the next 50 ky or much longer.

Projections of local climate and weather patterns are more uncertain. Climate models are generally relevant to larger geographic scales. However, the western United States is expected to experience higher temperatures and increased drought frequency at least into in the next century (Chapter 14 of IPCC 2013). It is difficult to determine what the longer-term impact of CO_2 levels will be in this region (specifically, the Utah area). However, the DTSA model assumes that Utah will not become sufficiently wetter and colder within the current interglacial period, to support lake rise to the elevation of Clive. An intermediate lake has not occurred in the Bonneville basin in the last 10 ka, and the future climate is expected to be hotter and drier. The justifications for these assumptions include:

- Lake Bonneville remained above the Clive elevation during most of the last glacial maximum based on the chronology and elevation of the lake shorelines.
- Intermediate lakes have been below the Clive elevation at least since the Gilbert shoreline (about 11.6 ka, Oviatt, 2014), which did not reach the elevation of Clive.
- The post-Gilbert lake level dropped to the current Great Salt Lake level then transgressed to near the Clive elevation at 10 ka followed by a return to the current lake level (Oviatt, 2014). This transgression and regression occurred during the transition from the glacial maximum to the start of the current interglacial period when melting ice sheets probably continued to supply significant quantities of runoff to the lake.
- An intermediate lake has not occurred in at least the past 10 ka, and current projections are for hotter and drier conditions for the American southwest until CO_2 levels return to

pre-industrial levels, suggesting that the arrival of an intermediate lake is very unlikely for the next 50 ky and possibly a lot longer.

The Lake Bonneville basin watershed is large and integrates runoff from the eastern Great Basin and transition region of the Colorado plateau. Long-term changes in evaporation and precipitation over a large region are required to sustain lake rise to the Clive elevation. These conditions may be expected to occur only with a return to glacial conditions given climate model forecasts of increased aridity for the southwest United States. Studies have been initiated of climate change risk to municipal water supplies in Utah using watershed hydrology models that explore temporal changes in average conditions (temperature, precipitation, runoff), and severe drought and water supply scenarios (for example, the Salt lake City Department of Public utilities, Bardsley et al., 2013). These types of studies are both prudent and timely but future projections of decade scale data are highly uncertain. Indeed, projection of the global climate change model results to regional models has been a developing topic in the succession of IPCC reports. Warming temperatures associated with anthropogenic climate effects will have significant impacts on the southwestern United States, but current drought projections do not exceed paleoclimate records of droughts over the last two millennia (Woodhouse et al., 2010; Morgan and Pomerleau, 2012). Multi-model ensemble studies of future climate projections from 16 global climate models show both decreases and increases in streamflow projections for the upper Colorado River Basin (Harding et al., 2012). Cook et al. (2010) suggest caution in projecting climate model projections for the arid Southwest. For the DTSA model, however, the lack of an intermediate lake since more than 10 ka, and the unlikely change in conditions necessary to produce an intermediate lake suggest that it is reasonable to model the return of an intermediate lake beyond 50 ky into the future.

The weight of evidence reviewed and summarized in the sequence of reports by the IPCC is considered to be substantive and persuasive and this information is included in the DTSA modeling. Thus, the following assumptions are made:

- CO_2 levels will continue to rise for the foreseeable future, or, at least, will not decrease below 300 ppm or pre-industrial levels.
- The IPCC and associated climate projection studies are valid, with a high degree of confidence. Their conclusion that the inception of the next glacial period will not occur for at least 50 ky is accepted and applied in the DTSA model;

Consequently, the next lake to reach the elevation of Clive is assumed to occur no sooner than 50 ky into the future.

4.0 Modeling Approach for the DTSA

The GoldSim systems analysis software (GTG, 2011), which was used to construct the Clive DU PA Model, is also used for the DTSA Model. The same Species list of contaminants, material properties, and site geometry are retained from the Clive DU PA Model v1.2.

The DU waste inventory for the start of deep time is taken from the Clive DU PA Model v1.2 at model year 10,000, using a deterministic simulation with the DU waste disposed below current grade. In doing so, the first 10 ky of contaminant fate and transport are captured. Whatever radioactivity remains in the lowest five waste layers (about the lowest 2.5 m of the embankment) at year 10,000 is used as the inventory for the DTSA at year 10,000.

The DTSA model is largely a heuristic representation of deep time. The underlying concepts are that a lake will return to the elevation of Clive at some point in the future, although when is extremely uncertain, and sedimentation will be sufficiently thick after the first lake recedes that radon flux will not be unacceptable. Contaminant fate and transport after 10 ky is not evaluated in the DTSA model, excepting radioactive decay and the ingrowth of progeny in the DU waste. The environment is modeled to evolve in only three ways:

- The depth of aeolian sediments in the vicinity of Clive increases over time,
- an intermediate lake deposits a layer of sediment as described in the *Deep Time Appendix to version 1.2 of the Modeling Report*, and
- the time of the return of an intermediate lake within the current cycle is modeled as a Poisson process, as described in the *Deep Time Appendix to version 1.2 of the Modeling Report*, but with a constraint that the first lake will not return for at least 50 ky (see Section 3.3).

As discussed in Section 2.0, the depth of sediment removed at the Clive location due to the effect of removal of sediment from wave action, and the residual material from the destroyed embankment are expected to be approximately equal, and their effects essentially cancel. Therefore, the thickness of residual embankment material and sediment overlying the disposed DU waste at the time when the first intermediate lake recedes will be effectively equivalent to the thickness of aeolian sediments deposited up until that point in time, represented by the rising elevation of the surrounding grade. The DTSA model calculates radon ground surface flux from radionuclides in the disposed DU waste buried beneath this layer.

4.1 Modeling of ^{222}Rn Flux

Radon-222 flux through the overlying sediment is calculated using the approach described in the Nuclear Regulatory Commission (NRC) Regulatory Guide 3.64 *Calculation of Radon Flux Attenuation by Earthen Uranium Mill Tailings Covers* (NRC, 1989). These equations were developed for estimating radon flux from uranium mill tailings buried under a monofill cover. For the DTSA model, an assumption is made that the material above the below-grade DU waste and the additional lake sedimentation is homogenous material with properties similar to those of the surrounding Unit 4 sediments. The use of an analytical model such as that described in NRC (1989) allows radon flux to be estimated through a homogeneous cover of varying thickness with minimal complexity.

Modeling of radon transport to the surface of the intact Federal DU Cell in the Clive DU PA Model v1.2 does not lend itself to such simplified analytical solutions, since the cover is constructed of layers with widely-varying properties. In that case, radon diffusive flux was integrated with other transport processes employing a column of well-mixed cells, allowing for the vertical redistribution of radionuclides over time throughout the disposal system by diffusive, advective, and biotic processes. Because the above-ground part of the Federal DU Cell is assumed to be dispersed by wave action from the first intermediate lake, these processes are not relevant to the DTSA except insofar as they affect radionuclide concentrations in the below-grade waste cells.

5.0 DTSA Results

The updated Clive DU PA Model vDTSA1 was run for 1,000 realizations to develop results for sediment thickness over time, related to aeolian and lake-derived deposition, and also radon flux as described above. The results of the 1,000 DTSA model realizations for the thickness of accumulated sediments within a modeling period of 200 ky are shown in

Figure 3. The model results displayed were considered sufficiently stable at 1,000 realizations.

As described in Section 3.3, the next lake to reach the elevation of Clive is assumed to occur no sooner than 50 ky into the future, so only aeolian deposition, at a constant rate, contributes to accumulation of sediments in the vicinity of Clive. Note that the embankment exists until the advent of the first lake, so the aeolian deposition thickness up to 50 ky is only sediment accumulation in the vicinity of Clive. When a lake reaches the Clive elevation, aeolian deposition is augmented by the deposition of lake-derived sediments. Because the number and timing of such lakes and the depth of deposited sediment are uncertain, the variability in sediment thickness after 50 ky in considerably greater than in the initial 50-ky modeling period. The change in the slope of the sediment thickness curve at approximately 90 ky reflects the deposition of sediment from a deep lake that might appear at this time within the 100-ky climate cycle.

The increasing depth of material covering the disposed DU waste over time will result in attenuation of radon flux. However, this rate of attenuation will be partly offset by the slowly increasing activity of the radioactive progeny of ^{238}U. Modeling results indicate that sediment accumulation overwhelms the influence of progeny ingrowth. This is revealed by inspection of the results of individual model realizations, where radon flux is always highest at the model time when the first intermediate lake recedes, and then decreases over time to the end of the modeling period. Hence, the time of peak radon flux is equivalent to the time when the first lake to reach the elevation of Clive (and destroy the embankment by wave action) has just receded from the location of the below-grade disposed DU waste.

The time when the first intermediate lake returns after 50 ky is modeled as a Poisson process and varies with each model realization. Therefore, the time of peak radon flux also varies with each realization. As shown in Figure 4, the likelihood that the first intermediate lake to reach Clive has appeared increases with time from 50 ky such that there is approximately a 95% probability that a lake will have appeared by approximately 90 ky. At that time the advent of an intermediate lake is overtaken by the probability that a deep lake will begin within this 100-ky climate cycle.

The radon flux over time is shown in Figure 5. Although radon flux will be highest at times closest to 50 ky, in most realizations a lake will not have occurred until closer to 60 ky. As described in relation to previous figures, the change in the slope of radon flux curve in Figure 5 reflects the deposition of sediment from a deep lake that appears at this time within the 100-ky climate cycle.

The peak of the mean radon flux shown in Figure 5 is approximately 1.7 pCi/m^2-s. The peak occurs in the DTSA model at about 61,000 yr.

Although the median and mean sediment thickness track closely, the mean radon ground surface flux is much larger than the median. This strongly skewed result for radon flux is a consequence of the nonlinearities inherent in the NRC radon ground surface flux calculation. These are equations (9) through (12) in NRC (1989), here reproduced without detailed explanation:

$$J_t = 10^4 R_t \rho_t E_t \sqrt{\lambda D_t} \tanh\left(x_t \sqrt{\lambda / D_t}\right)$$

$$b_t = \sqrt{\lambda / D_t}, \quad b_c = \sqrt{\lambda / D_c}$$

$$a_t = n_t^2 D_t [1 - (1-k) m_t]^2, \quad a_c = n_c^2 D_c [1 - (1-k) m_c]^2$$

$$J_c = \frac{2 J_t e^{(-b_c x_c)}}{1 + \sqrt{a_t / a_c} \tanh(b_t x_t) + \left[1 - \sqrt{a_t / a_c} \tanh(b_t x_t)\right] e^{(-2 b_c x_c)}}$$

The definitions of variables are available in the NRC Regulatory Guide (1989), but it is clear that these equations will produce a highly nonlinear result, J_c, which is the ground surface flux of radon. So, even though all the inputs to the calculation are essentially normal distributions, the complexity of dividing one by another, and involving powers (e.g. e^x) and hyperbolic tangent, produces a nonlinear result.

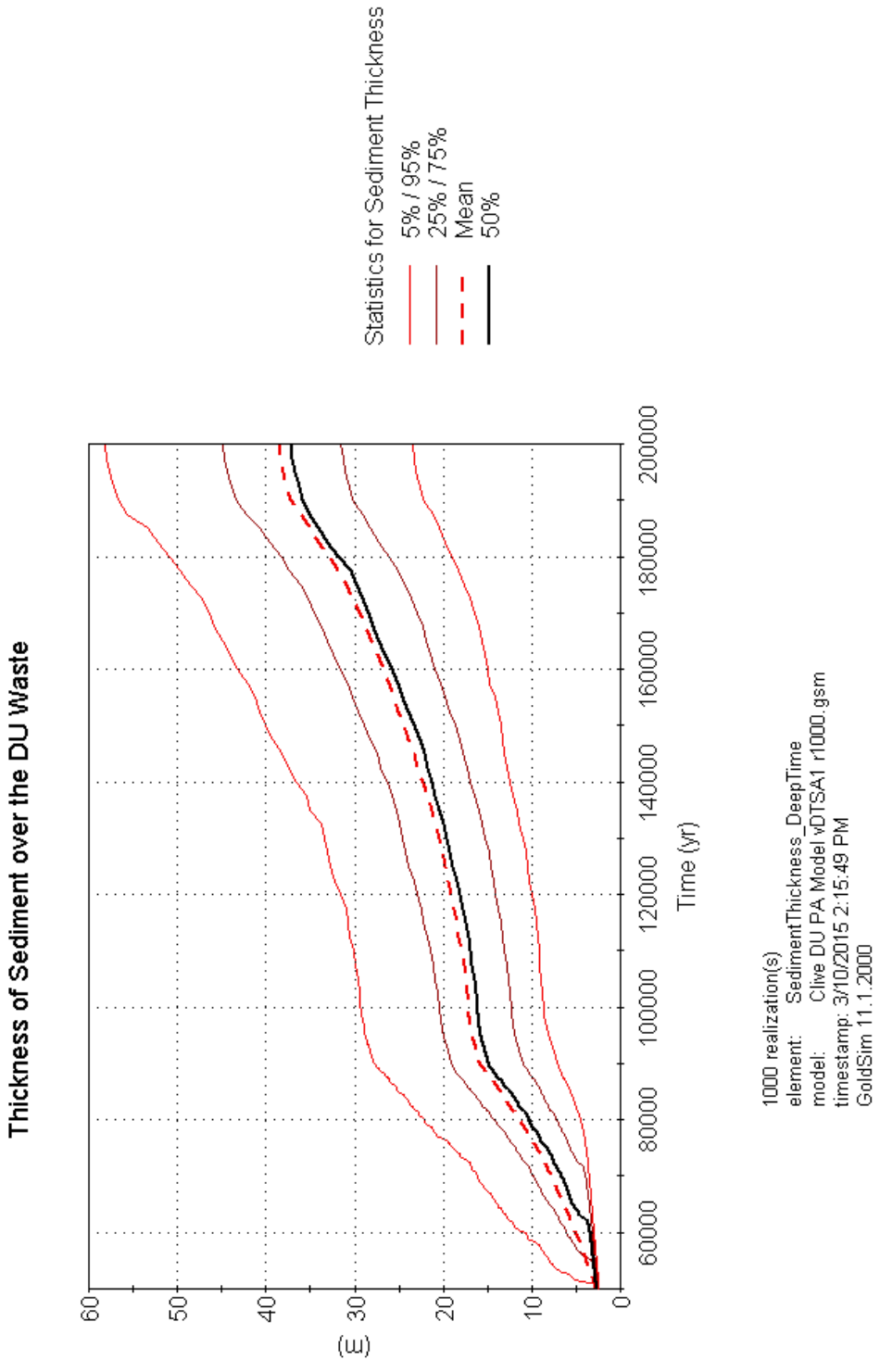

Figure 3. Evolution of Sediment Thickness in Deep Time

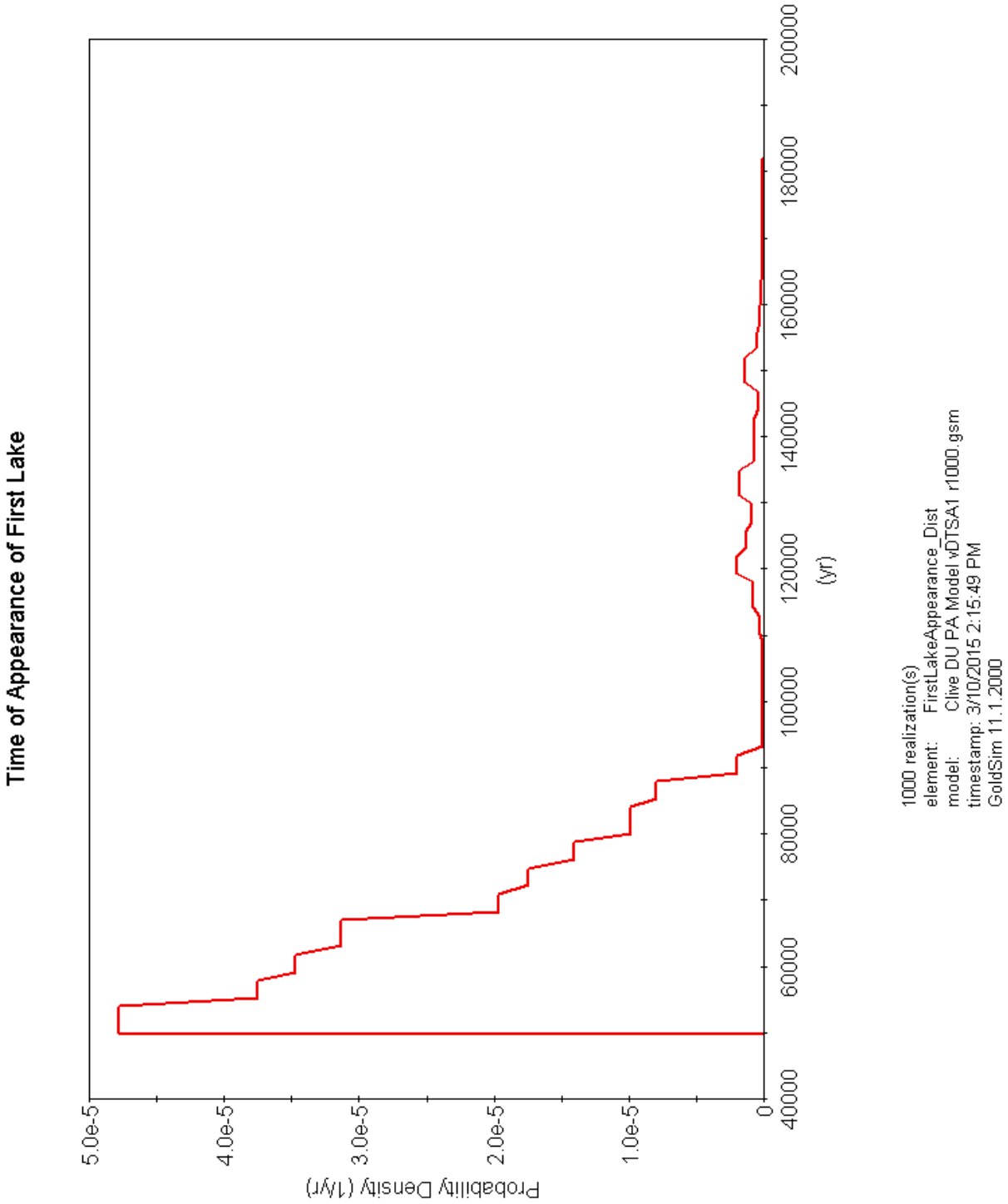

Figure 4. Time of appearance of first intermediate lake to reach the Clive elevation

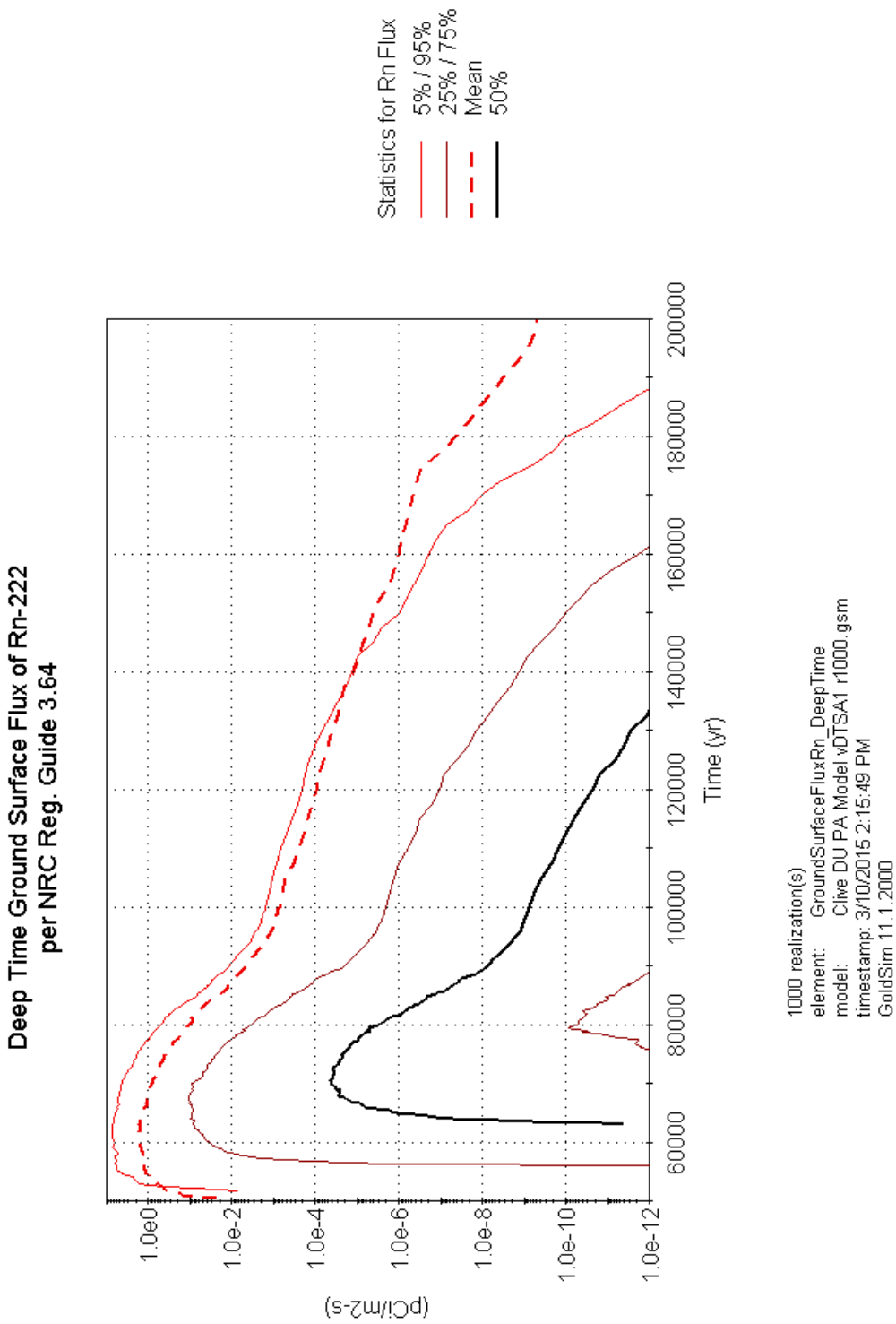

Figure 5. ^{222}Rn ground surface flux in deep time

References

ANL (Argonne National Laboratory), 2001. *User's Manual for RESRAD Version 6*, ANL/EAD-4, Argonne National Laboratory, prepared for the United States Department of Energy, Argonne, IL.

Bardsley, T., A. Wood, M. Hobbins, T. Kirkham, L. Briefer, J. Niermeyer, and S. Burian, 2013. Planning for an Uncertain Future: Climate Change Sensitivity Assessment toward Adaptation Planning for Public Water Supply, *Earth Interactions,* 17, Paper No. 23.

Cook, E.R., R. Seager, R.R. Helm Jr, R. S. Vose, C. Herweijer, and C. Woodhouse, 2010. Megadroughts in North America: Placing IPCC Projection of Hydroclimatic Change in a Long-Term Palaeoclimate Context, *Journal of Quaternary Science,* 25, Issue 1, 48-61.

Goudie, A.S., I., Livingstone, S. Stokes, 1997. *Aeolian environment, sediments, and landforms*, Wiley Interscience, 1997.

Harding, B.L., A.W. Wood, and J.R. Prarie, 2012. The Implications of Climate Change Scenario Selection for Future Streamflow Projection in the Upper Colorado River Basin, *Hydrol. Earth Syst. Sci, 16, 3989-4007.*

IAEA. The Safety Case and Safety Assessment for the Disposal of Radioactive Waste. Vienna, Austria: International Atomic Energy Agency; Specific Safety Guide No. SSG-23; 2012.

IPCC, 2013: Climate Change 2013: The Physical Science Basis. Contribution of Working Group I to the Fifth Assessment Report of the Intergovernmental Panel on Climate Change [Stocker, T.F., D. Qin, G.-K. Plattner, M. Tignor, S.K. Allen, J. Boschung, A. Nauels, Y. Xia, V. Bex and P.M. Midgley (eds.)]. Cambridge University Press, Cambridge, United Kingdom and New York, NY, USA.

Jewell, P.W. and K. Nicoll, 2011. Wind Regimes and Aeolian Transport in the Great Basin, U.S.A., *Geomorphology,* V. 129 1-13.

GTG (GoldSim Technology Group), 2011. *GoldSim: Monte Carlo Simulation Software for Decision and Risk Analysis*, http://www.goldsim.com

Mornan, C. and M. M Pomerleau, 2012. New Evidence for Extreme and Persistent Terminal Medieval Drought in California's Sierra Nevada, *J. Paleolimnol*, 47, 707-713.

Nelson, D.T., 2012. Geomorphic and Stratigraphic Development of Lake Bonneville's Intermediate Paleoshorelines during the Late Pleistocene, PhD Dissertation, University of Utah, 237 p.

Neptune and Company, Inc., 2014, *Final report the Clive DU PA Model*, Clive DU PA Model v 1.2, Neptune and Company In., (June 5, 2014).

Neptune and Company, Inc., 2015, *Neptune field studies, December, 2014, Eolian depositional history Clive Disposal Site*.

NRC (Nuclear Regulatory Commission), 1989. *Calculation of Radon Flux Attenuation by Earthen Uranium Mill Tailings Covers*, U.S. Nuclear Regulatory Commission, Office of Nuclear Regulatory Research, Task WM 503-4, June 1989.

Oviatt, C.G., and B. P. Nash, 2014, *The Pony Express Basaltic Ash: A Stratigraphic Marker in Lake Bonneville Sediments, Utah,* Miscellaneous Publication 14-1, Utah Geological Survey 10 p.

Oviatt, C.G., *Chronology of Lake Bonneville, 30,000 to 10,000 yr B.P*. Quaternary Science Reviews 110, 166-171, (2015).

Sack, D., 1999.The Composite nature of the Provo Level of Lake Bonneville, Great Basin, Western North America, *Quaternary Research,* v. 52, 316-327.

Schofield, I., P. Jewell, M. Chan, D. Currey, and M. Gregory, 2004.Shoreline Development, Longshore Transport and Surface Wave Dynamics, Pleistocene lake Bonneville, Utah, *Earth Surface Processes and Landforms,* v. 29, 1675-1690.

Tzedakis, P.C., E.W. Wolff, L.C. Skinner, v. Brovkin, d.A. Hodell, J.F. McManus, and D. Ranyaud, 2012a. Can We Predict the Duration of an Interglacial? Clim. Past 8, 1473-1485.

Tzedakis, P.C., J.E.T. Channel, D.A. Hodell, H.F. Kleiven, and L.C. Skinner, 2012b. Determining the natural length of the current interglacial, *Nature Geoscience,* 5, 138-141.

Woodhouse, C.A., D. M. Meko, G. M. MacDonald, D.W. Stahle, and E. R. Cook, 2010. A 1,200-year Perspective of 21st Century Drought in Southwestern North America, *Proc. Natl. Acad. Of Sciences,* 107, 21283-21288.

Appendix A

A.1 Clive Pit Wall Interpretation (C. G. Oviatt, unpublished data)